Synthesis and Evaluation of Diastereoisomers of 1,4,7-Triazacyclononane-1,4,7-tris-(glutaric acid) (NOTGA) for Multimeric Radiopharmaceuticals of Gallium

ARTICLE *in* BIOCONJUGATE CHEMISTRY · OCTOBER 2012

Impact Factor: 4.51 · DOI: 10.1021/bc300340g · Source: PubMed

CITATIONS
9

READS
21

8 AUTHORS, INCLUDING:

Takemi Rokugawa
Shionogi & Co., Ltd.
8 PUBLICATIONS **10** CITATIONS
SEE PROFILE

Yasushi Arano
Chiba University
217 PUBLICATIONS **2,059** CITATIONS
SEE PROFILE

Bioconjugate Chemistry

Article

pubs.acs.org/bc

Synthesis and Evaluation of Diastereoisomers of 1,4,7-Triazacyclononane-1,4,7-tris-(glutaric acid) (NOTGA) for Multimeric Radiopharmaceuticals of Gallium

Francisco L. Guerra Gomez,[†] Tomoya Uehara,[†] Takemi Rokugawa,[†] Yusuke Higaki,[†,‡] Hiroyuki Suzuki,[†] Hirofumi Hanaoka,[†] Hiromichi Akizawa,[§] and Yasushi Arano*[,†]

[†]Graduate School of Pharmaceutical Sciences, Chiba University, Chiba, Japan, 260-8675

[‡]School of Health Sciences, College of Medical, Pharmaceutical and Health Sciences, Kanazawa University, Ishikawa, Japan, 920-0942

[§]Health Science University of Hokkaido, 1757 Kanazawa, Tobetsu-cho, Ishikari-gun, Hokkaido, Japan 061-0293

Supporting Information

ABSTRACT: In the conventional synthesis of 1,4,7-tris-(glutaric acid)-1,4,7-triazacyclononane (NOTGA), four isomeric species are usually generated by the alkylation of 1,4,7-triazacyclononane with α-bromoglutaric acid diester. To estimate their biological efficacies as well as their stability and radiochemistry, the *RRR/SSS* and *RRS/SSR* NOTGA-^{t}Bu prochelators were isolated and the corresponding cyclic RGDfK (RGD) conjugates with triethylene glycol linkages were prepared. The *RRR/SSS* and *RRS/SSR* diastereomers were obtained in 69% and 17% yields, respectively. In the complexation reaction with $^{67}GaCl_3$, both diastereomers provided >98% radiochemical yields at pH 5 within 10 min when the reaction was conducted at room temperature. However, the *RRR/SSS* diastereomer exhibited more pH-sensitive radiochemical yields between pH 3.5 to 4.5. Despite their diasteromeric nature, both ^{67}Ga-labeled RGD-NOTGA remained stable during the apo-transferrin challenge, exhibiting similar affinity for integrin $\alpha_v\beta_3$ and biodistribution with predominant renal excretion. Similar tumor uptake was also observed in mice bearing U87MG tumor xenograft, which resulted in impressively high contrast SPECT/CT images. These findings indicate that the RGD-NOTGA conjugates of both diastereomers presented here possess equivalent biological efficacies and their combined usage would be feasible. It is worth noting that specific properties of a given biomolecule, cell expression levels of the corresponding target molecule, and presence or absence of a pharmacokinetic modifier would affect the structural differences between diastereomers on the ligand−receptor interactions and pharmacokinetics. Thus, the preparation of corresponding conjugates and evaluation of their chemical and biological performances still remains important for applying NOTGA to other biomolecules of interest using the diastereomerically pure NOTGA-^{t}Bu prochelator.

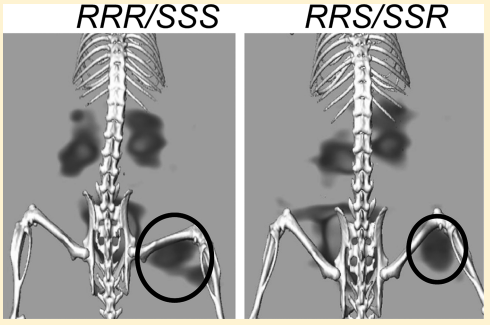

INTRODUCTION

Gallium radioisotopes are of great interest for molecular imaging. Gallium-68 (^{68}Ga) is a PET radioisotope available from long-lived ^{68}Ge/^{68}Ga generator systems allowing potentially cost-effective production of ^{68}Ga radiotracers far away from a cyclotron facility. Its physical half-life of 67.7 min is attractive for labeling low-molecular-weight probes with rapid pharmacokinetics.[1] Meanwhile, ^{67}Ga is a γ-emitter ($T_{1/2}$ = 3.3 d) currently used in the diagnosis of infection and inflammatory processes as well as tumor imaging by SPECT.[2,3]

For preparing $^{67/68}$Ga-based radiotracers, a macrocyclic chelator 1,4,7-triazacyclononane-*N*,*N*′,*N*″-triacetic acid (NOTA) is preferably used due to the formation of a hexadentate gallium complex of high thermodynamic (Log K = 30.98)[4] and kinetic stabilities arising from the good fit of the relatively small gallium cation in the cyclic cavity.[1] Moreover, this chelator has been efficiently radiolabeled with ^{68}Ga, even at room temperature.[5−7] Since the conjugation of targeting molecules to the carboxylic acids of NOTA compromises its coordination ability with Ga, several NOTA-based bifunctional chelating agents (BCA) with dissimilar functional groups in a pendant arm or on ethylene bridge have been developed.[6,8−10] Triazacyclononane (TACN) has been selected as the core of the scaffold containing phosphinic acid (triazacyclononane phosphinic acids; TRAP)[11,12] or glutaric acid (nonane triglutaric acid; NOTGA)[13,14] for multiattachment of biomolecules to the three pendant arms as a way to apply to the multimeric concept (Figure 1).

Recently, Singh et al.[14] exemplarily demonstrated that the binding affinity and tumor accumulation of a trivalent cyclic RGD peptide conjugated-NOTGA (^{68}Ga-**3**) increased with respect to its bivalent and monovalent counterparts. Similarly, Notni et al. reported that the targeting ability of the trivalent ^{68}Ga-TRAP(RGD)$_3$ was superior to that of the monovalent ^{18}F-Galacto-RGD.[12] However, one aspect to consider when

Received: June 26, 2012
Revised: October 7, 2012
Published: October 8, 2012

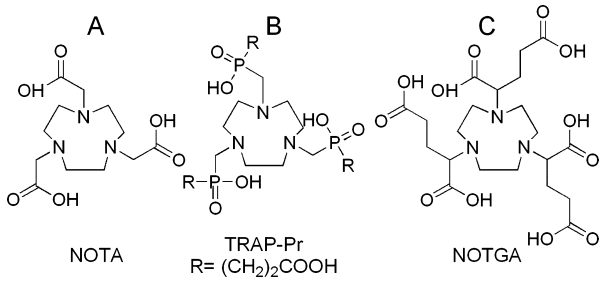

Figure 1. Structures of (A) NOTA and the NOTA-based BCAs, (B) TRAP, and (C) NOTGA. TRAP contains phosphinic acids, whereas NOTGA contains glutaric acids.

preparing NOTGA- and TRAP-based radiopharmaceuticals is the presence of chiral centers in their pendant arms leading to *RRR*, *SSS*, *RRS*, and *SSR* stereoisomers. In NOTGA, these stereoisomers are formed as a result of the alkylation of TACN with racemic (*R*/*S*) α-bromoglutaric acid diester (Figure 2),

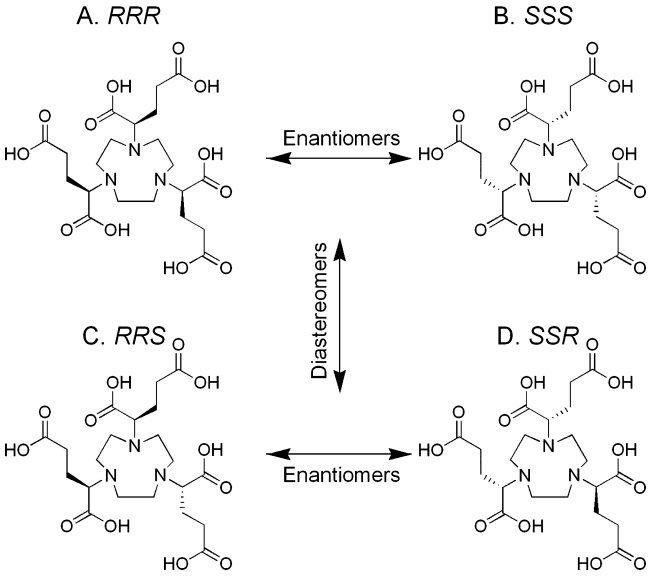

Figure 2. Structures of the isomeric forms of NOTGA. The *RRR* and *SSS*, as well as *RRS* and *SSR*, constitute enantiomers; while the pairs *RRR*/*SSS* and *RRS*/*SSR* are diastereomers.

which was also observed in the alkylation of tetraazacyclododecane,[15,16] where the *RRRR* isomer of gadolinium complex exhibited faster water exchange rate than the other isomers.[16] In TRAP ligands, the phosphorpous atoms become chiral upon coordination with the metal ion and four *RRR*, *SSS*, *RRS*, and *SSR* isomers are formed depending on the substituent.[11,17] A mixture of diastereomers, with differences in spatial orientation of the chelating unit or targeting molecules and physicochemical properties, might influence the biodistribution of the molecular probe.[18,19] In cases where radiopharmaceuticals can form distinct isomeric species, it is important to evaluate the individual product separately to ensure that they both possess good biological efficacy,[18] as well as stability and radiochemistry.

In TRAP-based radiolabeled probes, separation of a potential diastereomer can only be conducted after radiolabeling reaction. On the other hand, the isolation of diastereomers in NOTGA is feasible after alkylation of TACN, and diastereomerically pure conjugates can be obtained. In NOTGA-based radiolabeled probes, therefore, a diastereomerically pure $^{67/68}$Ga-labeled compound can be obtained without postlabeling purification by selecting a diastereomer of preferable chemical and biological performance. In the present study, pure diastereomers of NOTGA using RGDfK as the targeting molecule, were synthesized, and compared their performance in terms of radiochemical yields with $^{67}GaCl_3$, kinetic stability, affinity for integrin $\alpha_v\beta_3$, and biological behavior of each complex in normal and nude mice bearing U87MG tumor xenografts.

EXPERIMENTAL SECTION

General. All commercially obtained chemicals were of analytical grade and used without further purification. 9-Fluorophenylmethoxycarbonyl (Fmoc)-protected amino acids and H-Gly-2-Cl-Trt Resin were purchased from Watanabe Chemical Industries, Ltd. (Hiroshima, Japan). $^{67}GaCl_3$ was supplied by FUJIFILM RI Pharma Co., Ltd. (Tokyo, Japan). 1,4,7-Triazacyclononane (TACN) was purchased from Sigma Aldrich Chem. Co. (Milwaukee, WI, USA). Apo-transferrin (apo-Tf) Iron free was purchased from Nacalai Tesque Inc. (Kyoto, Japan). Reversed-phase HPLC was performed with a Cosmosil $5C_{18}$-AR-300 column (4.6 mm i.d. × 150 mm, Nacalai Tesque Inc.) at 1 mL/min with a gradient mobile phase starting from 90% A (0.1% aqueous trifluoroacetic acid (TFA) and 10% B (acetonitrile with 0.1% TFA) to 70% A and 30% B at 30 min. The eluent was monitored online with an UV−vis single-beam spectroscopy detector (L-7405, Hitachi Co. Ltd., Tokyo) coupled to a NaI(Tl) radioactivity detector (Gibi star, Raytest, Strubenhardt, Germany). TLC analyses was performed with silica plates (Silica gel 60 F_{254}, Merck Ltd., Tokyo) developed with MeOH/0.1 M $AcONH_4$ (1:1). Radioactivity was measured using a MiniGita Star Gamma TLC Scanner (Raytest) and an autowell γ counter (ARC-380M, Aloka, Tokyo). Mass spectrometry was carried out using an Agilent 6130 Series Quadrupole LC/MS electrospray system (Agilent Technologies, Tokyo) or MALDI TOF MS Kratos Axima CFR Plus (Shimadzu Corporation, Kyoto). ^1H, ^{13}C NMR spectra were recorded on a JEOL JNM-ECP-400 (400 MHz) spectrometer (JEOL Ltd., Tokyo).

(2-{2-[2-(9*H*-Fluoren-9-ylmethoxycarbonylamino)-ethoxy]-ethoxy}-ethoxy)-acetic acid (1) (Fmoc-TEG). 11-Amino-3,6,9-trioxaundecanoic acid (0.79 g, 3.79 mmol) and K_2CO_3 (1.04 g, 7.50 mmol) were dissolved in 5.8 mL of water and stirred at room temperature for 15 min after which *N*-(9-fluorenylmethoxycarbonyl) succinimide (1.28 g, 3.79 mmol) was added and the mixture was stirred for 24 h, while the progress of the reaction was monitored by TLC ($CHCl_3$/MeOH/AcOH, 5:1:0.06). The salt was filtered and the filtrate was washed with 3 × 3 mL of Et_2O, acidified to pH 1 using 3 N HCl, and the desired compound extracted with 5 × 5 mL of CH_2Cl_2. After removing the solvent in vacuo, the residue was purified with open column chromatography using silica gel and subsequent elution with $CHCl_3$/MeOH/AcOH (40:1:0.1) to afford Fmoc-TEG (1.19 g, 73%). ESI-MS, *m*/*z*: 430 $[M+H]^+$: Found 430.

Synthesis of Fmoc-TEG-c(-Arg(Pbf)-Gly-Asp(OtBu)-DPhe-Lys-) (2). Fmoc-TEG (0.16 g, 0.36 mmol), c(-Arg(Pbf)-Gly-Asp(O^{t}Bu)-DPhe-Lys-) (0.3 g, 0.33 mmol)[20] and 1-hydroxybenzotriazole monohydrate (HOBt, 0.049 g, 0.36 mmol) were dissolved in 13 mL of dimethylformamide (DMF) and cooled to −3 °C. Subsequently, 1-ethyl-3-(3-dimethylaminopropyl)-carbodiimide·hydrochloride (EDC, 0.21 g, 1.08 mmol) in 12 mL of DMF was added dropwise during 1 h under N_2 pressure. The reaction mixture was further stirred for 1 h and reacted overnight at room temperature. The solvent was removed in vacuo, and then, the residue dissolved in 100 mL of CH_2Cl_2, washed with 5% citric

dx.doi.org/10.1021/bc300340g | *Bioconjugate Chem.* 2012, 23, 2229−2238

acid (2 × 40 mL). The organic layer collected and dried over $MgSO_4$. After removing the solvent in vacuo, the residue was purified with open column chromatography using silica gel and subsequent elution with $CHCl_3$/MeOH (20:1) to obtained compound **2** as a white solid (0.22 g, 51%). ESI-MS, *m/z*: 1345 $[M+Na]^+$: Found 1345.

Synthesis of TEG-c(-Arg(Pbf)-Gly-Asp(OtBu)-DPhe-Lys-) (3). Fmoc-TEG-c(-Arg(Pbf)-Gly-Asp(OtBu)-DPhe-Lys-) (0.47 g, 0.35 mmol) was dissolved in 23 mL of 10% piperidine DMF solution and stirred for 2 h. After concentrating the solvent, Et_2O was added to the solution. The white precipitate was filtrated, washed alternatively with Et_2O and *n*-hexane, dried in vacuum overnight to obtain compound **3** as a yellow solid (0.30 g, 76%). ESI-MS, *m/z*: 1101 $[M+H]^+$: Found 1101.

1,4,7-Tris-(1-*tert*-butoxycarbonyl-3-benzyloxycarbony-propyl)-1,4,7-triazacyclononane (4) (NOTGA-^{t}Bu$_3$-Bz$_3$). (*R/S*) α-Bromoglutaric acid 1-*tert*-butyl ester 5-benzyl ester (1.3 g, 3.64 mmol)[21] was dissolved in 3.5 mL of acetonitrile and added dropwise to a solution of 1,4,7-triazacyclononane (0.142 g, 1.10 mmol) in 3.3 mL acetonitrile with K_2CO_3 (0.913 g, 6.62 mmol) during 2 h at 0 °C under N_2. The mixture was stirred at room temperature for 24 h. The reaction mixture was filtrated and the solvent was evaporated in vacuo. The residue was dissolved in dichloromethane (15 mL) and washed with 5% of $NaHCO_3$ (3 × 10 mL), and the organic layer was dried over $MgSO_4$. After removing the solvent in vacuo, the residue was purified with open column chromatography using silica gel and subsequent elution with chloroform/acetone (50:1) to afford compound **4** as a yellowish oil. *RRR/SSS* (0.637 g, 69%): ^{1}H NMR (400 MHz, $CDCl_3$), δ (ppm): 7.28−7.34 (m, 15H, Ph); 5.10 (s, 6 H, CH_2−Ph); 3.09−3.13 (t, 3H, N−CH); 2.68, 2.95 (d, *J* = 0.031, 12H, N-CH_2-CH_2-N); 2.53−2.42 (m, 6H, CH_2−COOBz); 1.82−2.03 (m-m, 6H, N-CH-CH_2); 1.43 (s, 27H, $C(CH_3)_3$). ^{13}C NMR (100 MHz, $CDCl_3$), δ (ppm): 173.37 (COOBzl); 172.59 (COO-tBu); 128.44, 128.48, 128.81, 136.34 (Ph); 81.11 (C-Me3); 67.58 (C-Ph); 66.46 (N-C); 54.55 (N-C-C-N); 31.59 (C-COO-Bzl); 28.58 (tBu); 25.58 (C-COO-Bzl). *RRS/SSR* (0.165 g, 17%): ^{1}H NMR (400 MHz, $CDCl_3$), δ (ppm): 7.26−7.34 (m, 15H, Ph); 5.09, 5.10 (d, 6 H, CH_2−Ph); 3.09−3.13 (m, 3H, N−CH); 2.58, 2.93 (d, *J* = 0.031, 4H, N-CH_2-CH_2-N), 2.70−2.84 (m, 8H, N-CH_2-CH_2-N); 2.44−2.51 (m, 6H, CH_2-COOBz); 1.82−2.02 (m-m, 6H, N-CH-CH_2); 1.43, 1.44 (d, 27H, $C(CH_3)_3$). ^{13}C NMR (100 MHz, $CDCl_3$), δ (ppm): 173.02, 173.13 (d, COOBzl); 172.30, 172.42 (d, COO-tBu); 128.10, 128.14, 128.46, 135.99 (Ph); 80.77, 80.79 (C-Me_3); 66.93 (C-Ph); 66.10, 66.27 (N−C); 54.29, 53.85, 53.54 (N−C−C−N); 31.02, 31.18 (C−COO−Bzl); 28.24 (tBu); 25.17, 25.33 (C−COO−Bzl). ESI-MS, *m/z*: 958 $[M+H]^+$, Found 958.

1,4,7-(α-Bromoglutaric Acid 1-*tert*-Butyl Ester 5-Benzyl Ester)-1,4,7-triazacyclononane (5, 6) (NOTGA-^{t}Bu$_3$). The *RRR/SSS* (0.57 g, 0.59 mmol) and *RRS/SSR* (0.15 g, 0.16 mmol) fractions were dissolved in methanol/water (5:1) and then 10% Pd/C (381 and 103 mg, respectively) was added portionwise. The mixtures were stirred for 12 h under H_2 atmosphere, then filtered over Celite, and evaporated to dryness to obtain compounds **5** and **6** as white solids. The products were used without further purification. *RRR/SSS* (408 mg, 96.4%). ^{1}H NMR (400 MHz, CD_3OD), δ(ppm): 3.69−3.70 (br, 3H, N−CH); 2.99−3.13 (br, 12H, N−CH_2−CH_2−N); 2.52−2.64 (br, 6H, CH_2−COOH); 2.06−2.19 (br, 6H, N−CH−CH_2); 1.51 (s, 27H, $C(CH_3)_3$). *RRS/SSR* (104 mg, 95%). ^{1}H NMR (400 MHz, CD_3OD), δ(ppm): 3.62−3.72 (br, 3H, N−CH); 2.87−3.22 (br, 12H, N−CH_2−CH_2−N); 2.44−2.81 (br, 6H, CH_2−COOH); 2.1.9−2.15 (br, 6H, N−CH−CH_2); 1.51 (s, 27H, $C(CH_3)_3$). ESI-MS, *m/z*: 688 $[M+H]^+$, Found 688.

NOTGA-(TEG-RGD)$_3$ (7). NOTGA-^{t}Bu$_3$ (*RRR/SSS*, 8.52 mg, 12.4 μmol; *RRS/SSR*, 10 mg, 14.5 μmol) was dissolved in dry CH_2Cl_2 (0.5 mL) and 0.3 equiv of 4-dimethylaminopyridine (DMAP), 3.5 equiv of TEG-c(-Arg(Pbf)-Gly-Asp(OtBu)-DPhe-Lys-), 3.6 equiv of 1-ethyl-3-(3-dimethylaminopropyl) carbodiimide·hydrochloride (EDC) dissolved in 0.5 mL of CH_2Cl_2 were added dropwise on an ice bath. After stirring at room temperature for 12 h under N_2, the solvent was evaporated in vacuo. The residue was dissolved in CH_2Cl_2 (10 mL), washed with 5% $NaHCO_3$ (3 × 7 mL), and dried over $MgSO_4$. After removing the solvent, the residue was taken up by a small amount of $CHCl_3$. The precipitate formed upon addition of excess of Et_2O was filtered and dried in vacuum overnight to obtain a yellow solid (*RRR/SSS*, 33.3 mg, 68.2%; *RRS/SSR*, 38.7 mg, 67.6%). ESI-MS, *m/z*: 1313 $[M+H]^{2+}$, Found 1313. After treatment with TFA/triethylsilane/H_2O (90:5:5) at room temperature for 3 h, the solvent was evaporated in vacuo and the precipitate formed upon addition of excess of Et_2O (*RRR/SSS*, 17.8 mg, 64.6%; *RRS/SSR*, 16 mg, 57.1%). ESI-MS, *m/z*: 1422 $[M+2H]^{2+}$, Found 1422.

Ga-NOTGA-(TEG-RGD)$_3$. NOTGA-(TEG-RGD)$_3$ (*RRR/SSS*, 0.8 mg, 0.28 μmol; *RRS/SSR*, 3 mg, 1.05 μmol) was dissolved in 500 μL of water, and 0.1 M $Ga(NO_3)_3$ solution (4.4 and 14.3 μL, respectively) was added. After 10 min heating at 70 °C, the pH was adjusted from 1.9 to 3.5 using 1 M sodium acetate and heated for another 30 min. The complex was purified by preparative HPLC and lyophilized to obtain Ga-NOTGA-(TEG-RGD)$_3$ (*RRR/SSS*, 0.7 mg, 85%; *RRS/SSR*, 2.67 mg, 87%). ESI-MS, *m/z*: 1455 $[M+2H]^{2+}$, Found 1455.

^{67}Ga-Radiolabeling. The complexation of ^{67}Ga by both diastereomeric pairs of ligands was studied regarding the reaction pH and time at r.t. $^{67}GaCl_3$ (10 μL, 1.5 MBq) in 0.05 M HCl was mixed with 10 μL of 0.5 M sodium acetate buffer pH 4−5.5. The mixtures were added to Eppendorf tubes containing 0.4 nmol of ligand in 20 μL of 0.25 M acetate buffer pH 3−5.5 to give final solutions of 0.25 M A.B, pH 3.5−5.5, and 10 μM of ligand concentration. The mixtures were incubated at 25 °C for 5, 10, and 15 min, and radiochemical yields were determined by Radio-TLC.

In Vitro Stability. ^{67}Ga-labeled complexes (*RRR/SSS*, *RRS/SSR*) were purified by RP-HPLC to remove unlabeled ligands. The radioactive peak was collected and the solvent was removed in vacuo. The residue was reconstituted in apo-transferrin (apo-Tf) solution (50 μM, 0.1 M carbonate buffer, pH 7.4) and incubated at 37 °C. Samples were withdrawn at 1, 3, and 6 h and analyzed by Radio-TLC (*n* = 3).

Binding Affinity to Integrin $\alpha_v\beta_3$. To evaluate the binding affinity of Ga-labeled compounds to integrin $\alpha_v\beta_3$, surface plasmon resonance (SPR) technology-based ProteOn XPR36 protein interaction array system (Biorad Laboratories Japan, Yokohama, Japan) was used. The SPR experiment was performed according to the manufacturer's instruction. In brief, human purified integrin $\alpha_v\beta_3$ (20 μg/mL, Chemicon International, Temecula, CA, USA) dissolved in 10 mM acetate buffer (pH 4.0) was immobilized on a ProteOn GLH sensor chip (Biorad Laboratories Japan) by standard amine coupling method. The Ga-NOTGA-(TEG-RGD)$_3$ complexes (*RRR/SSS*, *RRS/SSR*) at 10, 5, 2.5, and 1.25 μM concentrations and *c*(RGDfk) at 200, 100, 50, 25, and 12.5 μM as a positive control

in 10 mM Tris-HCl buffer (50 mM NaCl, 1 mM $MgCl_2$, 1 mM $MnCl_2$, pH 7.4) were injected simultaneously into the six horizontal channels of the chip. Kinetic analysis was performed by globally fitting curves describing a simple 1:1 biomolecular model to the set of five sensorgrams.

Cell Line. Human glioblastoma U87MG cells were grown in a 75 cm^2 tissue culture flask with canted neck (Becton, Dickinson and Company, Tokyo) in Dulbecco's Modified Eagle Medium (Sigma-Aldrich Japan K.K., Tokyo) supplemented with 10% fetal calf serum (FCS, Nippon Biosupply Center, Tokyo) and GIBCO BRL 1% penicillin−streptomycin (5000 unit-5000 μg/mL, Invitrogen, Life Technologies Japan Ltd., Tokyo), at 37 °C in a humidified atmosphere containing 5% CO_2.

Biodistribution Studies. Animal studies were conducted in accordance with institutional guidelines approved by the Chiba University Animal Care Committee. Male 6-week-old ddY mice[22] (Japan SLC, Inc., Shizuoka, Japan) were injected via tail vein with either *RRR/SSS* or *RRS/SSR* diastereomers of ^{67}Ga-NOTGA-(TEG-RGD)$_3$ (100 μL, 11.1 KBq, 10 μM ligand concentration). The animal were sacrificed and dissected at 30 min, 1 h, 3 h, and 6 h after administration. Tissues of interest were removed, weighed, and the radioactivity counts determined with an autowell gamma counter. The urine and feces were collected for 6 h and the radioactivity was also measured. Values were expressed as mean ± SD for a group of 3−5 animals.

BALBc nu/nu male mice (Japan SLC, Inc., Shizuoka, Japan) of 6 weeks old, weighing 18−20 g, were xenografted by subcutaneous (s.c.) injection of U87MG human glioblastoma cells (5×10^6 cells/80 μL of culture medium) into their right hind legs. The mice were subjected to biodistribution studies as well as SPECT/CT imaging studies when the tumor volume reached 100−300 mm^3.

Biodistribution studies were also conducted in male BALBc nu/nu mice bearing U87MG xenografts 30 min after administration of each radiotracer (n = 4). The integrin $\alpha_v\beta_3$ specificity was estimated by coinjection of either *RRR/SSS* or *RRS/SSR* diastereomers of ^{67}Ga-NOTGA-(TEG-RGD)$_3$ (100 μL, 11.1 KBq, 10 μM ligand concentration) and c(RGDyV) peptide (3 mg/kg mouse body weight) into mice bearing U87MG tumors. The animals were sacrificed and dissected at 2 h after administration (n = 4).

Small Animal SPECT/CT Imaging Studies. SPECT/CT images were taken 30 min after administration of either *RRR/SSS* or *RRS/SSR* diastereomers of [^{67}Ga]-NOTGA-(TEG-RGD)$_3$ (100 μL, 4.5 MBq, 10 μM ligand concentration) to male BALBc nu/nu mice bearing U87MG xenografts from the tail vein (n = 3). The mice were anaesthetized with 1−2% (v/v) isoflurane (DS Pharma Animal Health, Osaka, Japan) and positioned on the animal bed where anesthesia was continuously delivered via a nose cone system. SPECT imaging and X-ray CT imaging were performed by use of small animal SPECT/CT system (FX-3200, Gamma Medica Inc., CA) equipped with a five pinhole (0.5 mm) collimator. Data acquisition was performed for 64 min at 60 s per projection with stepwise rotation of 64 projections over 360°.

Statistical Analysis. Quantitative data were expressed as means ± SD. Means were compared using unpaired two-tailed Student's t test. P values <0.05 were considered statistically significant.

RESULTS

Synthesis. TACN was alkylated with (*R*/*S*) α-bromoglutaric acid 1-*tert*-butyl ester 5-benzyl ester[10,21,23] in acetonitrile and potassium carbonate at room temperature to obtain the fully protected NOTGA-^{t}Bu$_3$-Bz$_3$ **4** (Scheme 1). Purification was carried out using silica-gel column chromatography and a mixture of chloroform and acetone as the mobile phase. Two fractions (a major fraction of 69% and the following of 17%) were verified to be the target compound by mass spectrometry. Structure assignment was possible by ^{1}H NMR and ^{13}C NMR, which provides deeper insights into their structural differences (Supporting Information). Focusing on the chiral carbon resonance (label b in Figure 1S), a singlet was observed in the 69% fraction Figure 1S A) indicating equivalent carbons, and a doublet in the 17% fraction indicating the presence of two chemically nonequivalent carbons (Figure 1SB). The 69% fraction was assigned to the *RRR/SSS* diastereomeric pair and the 17% to the *RRS/SSR*.

In order to evaluate the differences of both diastereomeric pairs, each fraction was treated separately. After debenzylation by palladium-catalyzed hydrogenolysis, the diastereomeric orthogonally protected NOTGA-^{t}Bu$_3$ prochelator were obtained in quantitative yields.

The peptide substituent was prepared using an Fmoc chemistry to introduce the TEG spacer in the lysine side chain of c(RGDfK) in 50% yield. The prochelators of NOTGA-^{t}Bu$_3$ were then conjugated to the partially protected TEG-c(-Arg(Pbf)-Gly-Asp(OtBu)-DPhe-Lys-) by in situ activation using the standard EDC-based coupling method followed by complete removal of all protecting groups to obtain the desired ligands at moderate yields after HPLC purification (>95% purity).

Radiochemistry. The *RRR/SSS* and *RRS/SSR* pairs of NOTGA-(TEG-RGD)$_3$ were radiolabeled with ^{67}Ga and the resulting complexes were analyzed by HPLC (Figure 3). In both cases, a single peak was observed and the retention time of the *RRR/SSS* was 24.5 min, slightly longer than that of *RRS/SSR* (24.3 min). In both cases, their retention times were identical to those of the corresponding nonradioactive gallium complexes verified by mass spectrometry.

Formation kinetics as a function of pH is presented in Figure 4. In both cases, radiochemical yields were low under acidic conditions (pH 3.5) and quantitative at more basic pH 5 where the time variation of the radiochemical yield was essentially the same for both pairs (Figure 4B) and complete radiolabeling with more than 98% yield was attained after 10 min of reaction. Interestingly, while *RRR/SSS* was preferentially labeled at pH 5, the *RRS/SSR* was pH-independent from pH 4 to 5.5 (Figure 4A). Under the present condition, the specific activity of the ^{67}Ga-labeled compounds was 4500 Mq/μmol.

In Vitro Stability. The kinetic stability of [^{67}Ga]-NOTGA-(TEG-RGD)$_3$ diastereomeric pairs purified by HPLC in order to remove the excess ligand was estimated in an apo-transferrin challenge (Table 1). After 6 h of incubation at 37 °C, more than 98% of the radioactivity was still bound to the NOTGA tripeptide conjugates of both pairs.

Binding Affinity. The binding kinetics of the two diasteromeric gallium complexes of NOTGA-(TEG-RGD)$_3$ to $\alpha_v\beta_3$ integrin was estimated with the SPR technology using a monovalent c(RGDfK) as a reference (Table 2). Both diastereomeric trivalent complexes exhibited higher association and lower dissociation rates than that of a monovalent c(RGDfK) with the rate constants similar each other. As a result, both trivalent complexes showed 10-fold higher dissociation constant values (K_D) than that of monovalent c(RGDfK).

In Vivo Experiments. The results of the biodistribution studies of [^{67}Ga]-NOTGA-(TEG-RGD)$_3$ in normal mice at

Scheme 1. Synthesis of NOTGA-(TEG-RGD)$_3$[a]

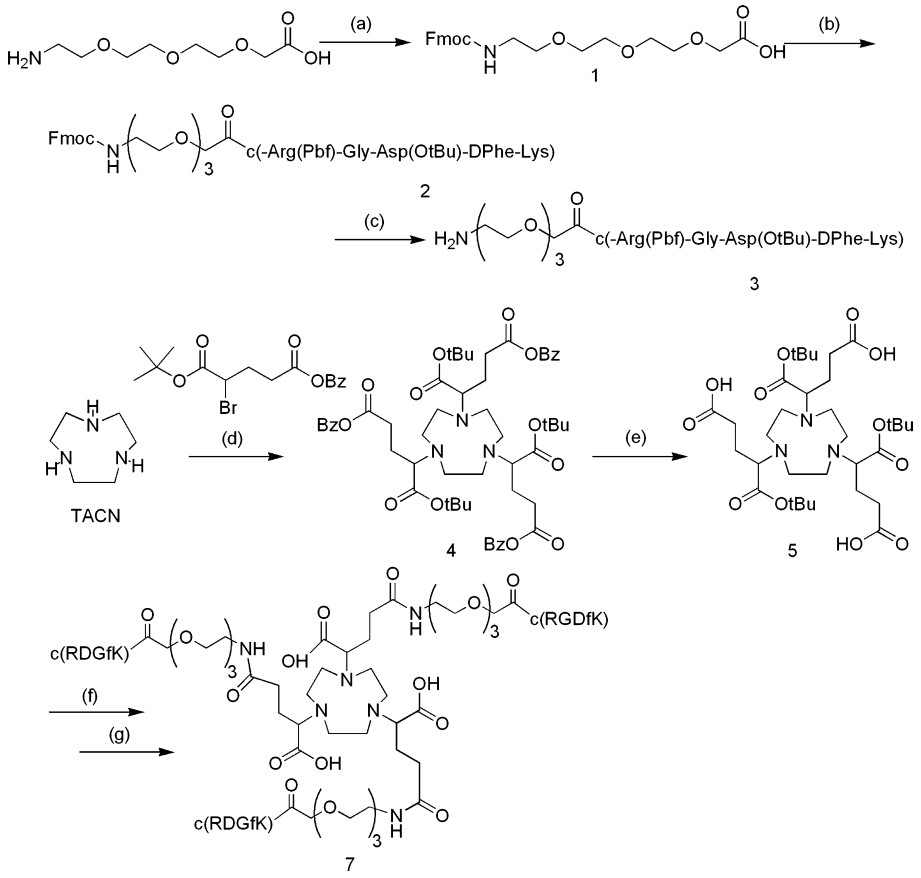

[a](a) Fmoc-O-Su, K_2CO_3, H_2O; (b) c(-Arg(Pbf)-Gly-Asp(O^{t}Bu)-DPhe-Lys-), WSCI/HCl, HOBt, DMF; (c) 10% piperidine/DMF; (d) 1,4,7-triazacyclononane, K_2CO_3, MeCN; (e) 10%Pd/C MeOH,H_2O; (f) H_2N-TEG-c(R(Pbf)GD(O^{t}Bu)fK), WSCI·HCl, DIMAP, CH_2Cl_2; (g) TFA/Water/Et_3Si.

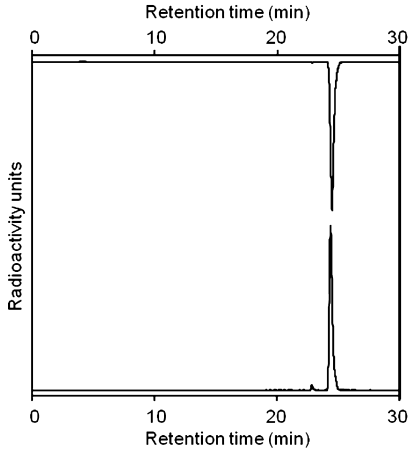

Figure 3. HPLC radiochromatograms of ^{67}Ga-NOTGA-(TEG-RGD)$_3$. The *RRR/SSS* diastereomer (top) was eluted at 24.5 min, slightly longer than that of the *RRS/SSR* counterpart (bottom, 24.3 min).

30 min, 1 h, 3 h, and 6 h after administration are shown in Table 3 (*RRR/SSS*) and Table 4 (*RRS/SSR*). No significant differences were observed in the uptake of both diastereomers in almost all organs and tissues. These profiles were characterized by rapid blood clearance with low accumulation in the liver, and the majority of the radioactivity was localized in the kidneys. Both radioligands were excreted in the urine with a small amount in feces. Although in absolute terms the uptake in

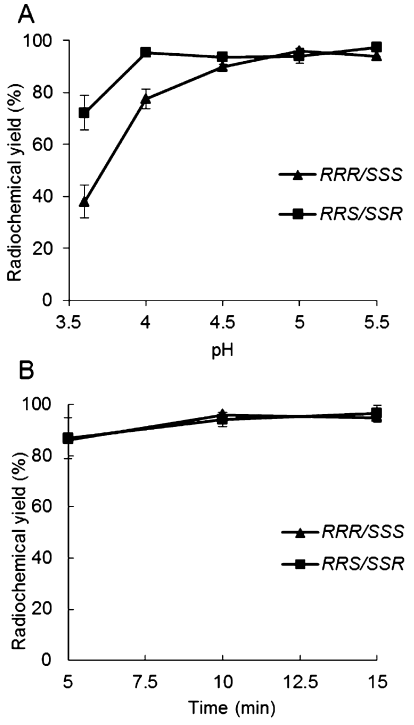

Figure 4. Radiochemical yields of each diastereomer of ^{67}Ga-NOTGA-(TEG-RGD)$_3$ (*RRR/SSS*, squares; and *RRS/SSR*, triangles) (A) at different pH values for 10 min and (B) different reaction times at pH 5.0.

dx.doi.org/10.1021/bc300340g | *Bioconjugate Chem.* 2012, 23, 2229−2238

Table 1. Stability of ^{67}Ga-NOTGA-(TEG-RGD)$_3$ Diastereomers against Apo-Transferrin[a]

time (h)	percent of intact radiolabeled complex	
	RRR/SSS	*RRS/SSR*
1	98.6 ± 0.2	98.9 ± 0.4
3	98.9 ± 0.3	98.3 ± 0.9
6	98.0 ± 0.4	98.4 ± 0.2

[a]Results are expressed as mean ± SD of three experiments.

the intestines was very low, a slight tendency of the *RRR/SSS* to be excreted through the intestinal tract can be noted. Its intestine accumulation was significantly higher at 1, 3, and 6 h p.i. Likewise, relatively higher radioactivity in feces and lower radioactivity in urine for the *RRR/SSS* were observed.

Figure 5 shows the biodistribution studies of [^{67}Ga]-NOTGA-(TEG-RGD)$_3$ (*RRR/SSS* and *RRS/SSS*) at 30 min postinjection to nude mice bearing U87MG xenografts. The biodistribution profiles of both diastereomeric pairs were characterized by rapid blood clearance and high tumor uptake with comparatively low accumulation in nontarget organs and renal excretion pathway. In agreement with the studies in normal mice, the uptakes of the diastereomeric pairs in organs of interest were comparable. Tumor uptakes were 4.40 ± 0.38 and 4.77 ± 0.76%ID/g ($p < 0.05$) for *RRR/SSS* and *RRS/SSR*, respectively. Tumor to organ ratios (Figure 5B) were high for blood and muscle, moderate for the liver, and much lower for the kidney. A combination of slightly higher tumor and lower blood uptakes led to a statistically significantly higher tumor to blood ratio for the *RRS/SSR* pair. When the radiolabeled probes were coinjected with a high amount of RGDyV, tumor accumulation was significantly decreased ($p < 0.05$) to 0.82 ± 0.17 and 0.68 ± 0.2%ID/g at 2 h p.i. (*RRR/SSS* and *RRS/SSR*, respectively), demonstrating integrin $\alpha_v\beta_3$ targeting specificity (Figure 6).

SPECT/CT imaging studies were performed for both *RRR/SSS* and *RRS/SSS* diastereomers of [^{67}Ga]-NOTGA-(TEG-RGD)$_3$

Table 2. Kinetic Binding Constants of ^{67}Ga-NOTGA-(TEG-RGD)$_3$ (*RRR/SSS* and *RRS/SSR*), c(RGDfK) to Integrin $\alpha_v\beta_3$ Determined Using the SPR Technology

analyte	K_a (1/Ms)	K_d (1/s)	K_D (M)
RRR/SSS	$1.13 \times 10^5 \pm 6.8 \times 10^3$	$8.03 \times 10^{-3} \pm 1.7 \times 10^{-4}$	$7.13 \times 10^{-8} \pm 4.5 \times 10^{-9}$
RRS/SSR	$0.94 \times 10^5 \pm 5.3 \times 10^3$	$8.12 \times 10^{-3} \pm 1.6 \times 10^{-4}$	$8.64 \times 10^{-8} \pm 4.9 \times 10^{-9}$
c(RGDfK)	$2.57 \times 10^4 \pm 6.1 \times 10^3$	$1.38 \times 10^{-2} \pm 6.2 \times 10^{-4}$	$5.37 \times 10^{-7} \pm 2.7 \times 10^{-7}$

Table 3. Biodistribution of *RRR/SSS* Diastereomer of ^{67}Ga-NOTGA-(TEG-RGD)$_3$ in Normal Mice[a]

	RRR/SSS			
organ	30 min	1 h	3 h	6 h
blood	0.61 ± 0.13	0.16 ± 0.02	0.07 ± 0.02	0.09 ± 0.02
liver	1.27 ± 0.22	1.32 ± 0.15	1.49 ± 0.32	1.50 ± 0.30
spleen	2.09 ± 0.35	1.26 ± 0.12	1.32 ± 0.21	1.77 ± 0.56
kidneys	5.82 ± 1.22	5.04 ± 1.15	3.48 ± 0.54	3.00 ± 0.43
pancreas	1.06 ± 0.19	0.72 ± 0.09	0.65 ± 0.10	0.66 ± 0.13
heart	1.00 ± 0.07	0.69 ± 0.05	0.65 ± 0.09	0.73 ± 0.11*
lung	2.52 ± 0.33	1.41 ± 0.11	1.08 ± 0.37	1.25 ± 0.47
muscle	0.84 ± 0.14	0.55 ± 0.12	0.51 ± 0.07	0.52 ± 0.04
stomach[c]	0.63 ± 0.06	0.74 ± 0.16	0.56 ± 0.13	0.47 ± 0.14
intestines[b,c]	2.98 ± 0.54	3.67 ± 0.27**	5.23 ± 0.80*	4.44 ± 0.26**
urine[c]				63.22 ± 6.83
feces[c]				4.25 ± 1.30

[a]Data expressed as %ID/g ± SD ($n = 5$). [b](* $p < 0.05$, ** $p < 0.01$). [c]Expressed as %ID.

Table 4. Biodistribution of *RRS/SSR* Diastereomer of ^{67}Ga-NOTGA-(TEG-RGD)$_3$ in normal mice[a]

	RRS/SSR			
organ	30 min	1 h	3 h	6 h
blood	0.58 ± 0.18	0.19 ± 0.02	0.09 ± 0.03	0.08 ± 0.02
liver	1.22 ± 0.12	1.19 ± 0.07	1.56 ± 0.38	1.33 ± 0.19
spleen	1.42 ± 0.59	1.20 ± 0.17	1.40 ± 0.06	1.57 ± 1.17
kidneys	5.38 ± 0.89	4.74 ± 0.87	3.58 ± 0.39	3.04 ± 0.28
pancreas	0.85 ± 0.07	0.69 ± 0.03	0.71 ± 0.09	0.58 ± 0.11
heart	0.93 ± 0.16	0.73 ± 0.08	0.73 ± 0.09	0.55 ± 0.05*
lung	1.94 ± 0.53	1.36 ± 0.16	1.33 ± 0.35	1.00 ± 0.04
muscle	1.22 ± 0.91	0.55 ± 0.04	0.55 ± 0.06	0.62 ± 0.17
stomach[c]	0.59 ± 0.06	0.63 ± 0.11	0.61 ± 0.11	0.40 ± 0.02
intestines[b,c]	2.59 ± 0.35	3.00 ± 0.27**	4.10 ± 0.62*	2.90 ± 0.38**
urine[c]				71.52 ± 2.64
feces[c]				2.24 ± 0.89

[a]Data expressed as %ID/g ± SD ($n = 5$). [b](* $p < 0.05$, ** $p < 0.01$). [c]Expressed as %ID.

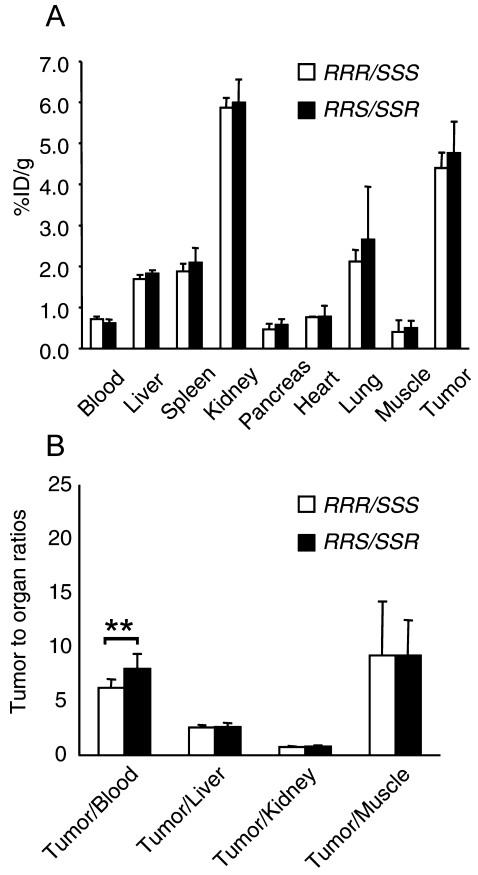

Figure 5. (A) Biodistribution of ^{67}Ga-NOTGA-(TEG-RGD)$_3$ in tumor-bearing male nude mice at 30 min after intravenous injection of 11.1 KBq of *RRR/SSS* (white) or *RRS/SSR* (black). (B) The tumor to organ ratios of the ^{67}Ga labeled conjugates. Data expressed as %ID/g ± SD (n = 4, ** p < 0.01).

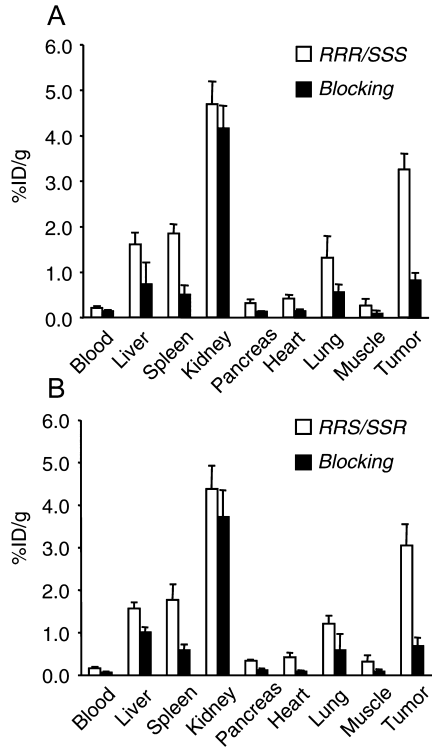

Figure 6. Biodistribution data in tumor-bearing male nude mice at 2 h after administration of ^{67}Ga-NOTGA-(TEG-RGD)$_3$ with (black) and without (white) the presence of an excess of RGDyV. (A) *RRR/SSS*; (B) *RRS/SSR*. Data expressed as %ID/g ± SD (n = 4).

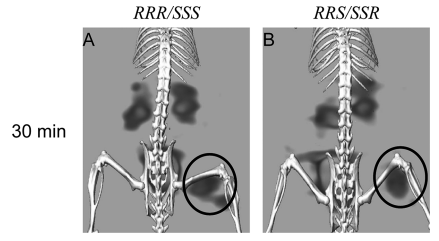

Figure 7. SPECT/CT images of U87MG tumor-bearing male nude mice after 30 min of i.v. injection of 4.5 MBq of each diastereomer of [^{67}Ga]-NOTGA-(TEG-RGD)$_3$. (A) *RRR/SSS* and (B) *RRS/SSR*. Images were shown at the same signal intensity scale.

using nude mice bearing U87MG xenografts (Figure 7). Tumors were clearly visualized as early as 30 min after administration. Radioactivity was concentrated in the kidneys and bladder. Impressively, nonspecific accumulation in liver or bowel was not observed, resulting in high-contrast images.

DISCUSSION

The cyclic RGD peptides have been widely study as a targeting molecule due to its high affinity for integrin $\alpha_v\beta_3$ overexpressed during tumor angiogenesis.[24] It has also been well recognized that in vitro binding affinity and in vivo tumor targeting ability of multimeric RGD peptides are enhanced due to the multivalent effect and the enriched local RGD concentration.[24−28] Moreover, it has been demonstrated that the spacer units of appropriate length and hydrophilicity between a radiometal chelate and each RGD motif increase avidity of the radiotracers and simultaneously may act as pharmacokinetic modifiers to improve pharmacokinetics of the radiotracer.[24,29,30]

The preparation of NOTA-based radiopharmaceuticals was conducted according to the procedure reported previously.[13,14] In brief, the synthesis of the orthogonally protected prochelator NOTGA-^{t}Bu$_3$, followed by conjugation of the bioactive molecules to each carboxylic acid of the pendant arm and final deprotection. Since racemic (*R*/*S*) α-bromoglutaric acid 1-*tert*-butyl ester 5-benzyl ester was used in the alkylation of TACN, intermediate **4** exists in different isomeric forms,[15,16] *RRR*, *SSS*, *RRS*, and *SSR* (Figure 2). The *RRR* and *SSS* isomers constitute enantiomers, as supported by similar MS and ^{13}C NMR spectra. Further isolation was not possible by the conventional methods. In ^{13}C NMR, since the three chiral carbons in *RRR/SSS* are equivalent, this pair was assigned to the 69% fraction with a single resonance. Similarly, two different carbons (*R*, *S*) are present in *RRS/SSR* and were associated with the doublet observed in the 17% fraction, as also observed in the tetraazacyclodecane analogue.[16]

It should be mentioned that, besides the isomerism in NOTGA ligands coming from the chiral carbon in the pendant arms, NOTA-based complexes are chiral depending on the orientation of the pendant arms around the metal center (Λ: clockwise or Δ: anticlockwise) and the relative puckering of the ethylenediamine subunit chelate rings ($\delta\delta\delta$ or $\lambda\lambda\lambda$ conformers)[31,32] in the case of gallium, only the enantiomeric $\Delta(\lambda\lambda\lambda)/\Lambda(\delta\delta\delta)$ combination was observed.[31] Therefore, each *RRR/SSS* and *RRS/SSR* of Ga-NOTGA diastereomeric pair may further exist as the enantiomeric combinations $\Delta(\lambda\lambda\lambda)$-*RRR*/$\Lambda(\delta\delta\delta)$-*SSS* or $\Delta(\lambda\lambda\lambda)$-*SSS*/$\Lambda(\delta\delta\delta)$-*RRR*, as well as $\Delta(\lambda\lambda\lambda)$-*RRS*/$\Lambda(\delta\delta\delta)$-*SSR*

dx.doi.org/10.1021/bc300340g | *Bioconjugate Chem.* 2012, 23, 2229−2238

or Δ(λλλ)-*SSR*/Λ(δδδ)-*RRS*. Nevertheless, both diastereomeric ligands provided gallium complexes of high inertness, indicating good retention of the metal inside the complex cavity.

^{67}Ga radiolabeling was performed at room temperature as previously reported for NOTA and its derivatives.[5−7] The reaction condition allowed assessing the differences in the complexation ability of the diastereomeric ligands that otherwise would be suppressed by heating. Lower radiochemical yields under acidic conditions were also found by Singh et al.[14] when labeling NOTGA and its disubstituted parent, in comparison to the monosubstituted and the *p*-SCN-Bn-NOTA RGD conjugates, possibly due to steric hindrance caused by the three substituents. On the other hand, pH 5 was found optimal for labeling NODAGA-RGD with ^{68}Ga,[33] and a study of the Ga-NOTA formation in acetate solutions found faster reaction rates at higher pH.[34] Intriguingly, the *RRS*/*SSR* was almost pH-independent from pH 4 to 5.5. A hypothesis to account for this observation would be related to the formation mechanism of the Ga-NOTA complex and the structural differences between the diastereomers. It has been reported that complexation of NOTA and other polyazamycrocycles containing pendant arms proceed in two steps. The first step comprises a fast formation of a monoprotonated intermediate species in which the metal ion is outside of the macrocyclic cage and coordinated to the three peripheric carboxylate oxygen atoms. The ring nitrogen atoms remain unbound and the proton would be attached to one of them. In the second step, deprotonation takes place followed by migration of the metal to inside the cavity where it also becomes coordinated to the nitrogen atoms.[35] Due to electrostatic repulsion between the nitrogen's proton and the metal, removal of the proton is considered to be the rate-determining step.[34,36,37] It has been proposed that this is an OH-catalyzed deprotonation,[34−37] explaining the faster complexation at higher pH. It has also been proposed that the migration of the proton from the NH^+ group to a carboxylate facilitates the accessibility with respect to OH^- ions.[37] In either case, the *RRS*/*SSR* conformation might facilitate access of the OH^- ions to the nitrogen-bound proton or the proton migration to the carboxylate, making the complexation less pH-dependent.

To further estimate the differences between the two diastereomers, the binding affinity of the two gallium complexes of NOTGA-(TEG-RGD)$_3$ to $\alpha_v\beta_3$ integrin were estimated by SPR assay and found that the structural differences in the NOTGA diastereomers presented here do not affect the interaction with the targets (Table 2). The binding to $\alpha_v\beta_3$ integrin is strongly dependent on the molecular design of multimeric RGD probes. There are two factors underneath the enhanced target affinity: multivalency and enhanced local RGD concentration. Although the local concentration factor is innate in all multimeric probes, an appropriate distance between each of two sets of cyclic RGD motifs is required to achieve multivalency.[24,38,39] In this design, the triethylene glycol spacer was inserted to provide a distance between the three carboxylates in NOTGA and the lysine side chains of the RGD motifs of 37 bonds. According to the previous study,[38] the distance between the two cyclic RGD motifs of [^{67}Ga]-NOTGA-(TEG-RGD)$_3$ would be suitable for simultaneous $\alpha_v\beta_3$ integrin binding. In addition, Syngh et al. reported that a trimeric RGD linked to NOTGA showed enhanced tumor uptake and retention compared with monomeric RGD counterpart, due to the multivalent effect partially.[14] From these findings, a combination of multivalency and enhanced local RGD concentration might be attributable to higher targeting capabilities of [^{67}Ga]-NOTGA-(TEG-RGD)$_3$, reflected in a binding affinity 10-folder higher than that of the monovalent cRGDfK. Thus, both diastereomers might act as trivalent compounds and the spatial arrangement of the RGD motifs in each complex would be equivalent with respect to binding affinity to $\alpha_v\beta_3$ integrin.

No significant differences were also observed in the biodistribution of the ^{67}Ga labeled diastereomers (Tables 3 and 4, Figure 5). Both exhibited rapid blood clearance and renal excretion in normal and nude mice bearing U87MG tumors. The high renal uptake was consistent with previous studies of other multimeric RGD peptides.[14,26,40−42] It was reported that endothelial cells of the glomeruli vessels in the kidneys express integrin $\alpha_v\beta_3$,[43] which could partially explain the observation. The presence of three guanidine groups in the trivalent RGD conjugate would increase positive charge, which may have facilitated reabsorption in proximal renal tubular cells.[26,27,43,44] While both diastereomers exhibited similar biodistribution, the elution order of the diastereomers from HPLC (Figure 3; *RRS*/*SSR* followed by *RRR*/*SSS*) suggests that a small difference in the lipophilicity between the two may be responsible for the slight tendency of the *RRR*/*SSS* to be excreted through the intestinal tract, though the excretion route is minimal. The similar affinity for integrin $\alpha_v\beta_3$ along with similar pharmacokinetics of the diastereomers resulted in similar tumor accumulation of the two compounds (Figure 5), yielding SPECT/CT images of high contrast as shown in Figure 7.

The longer-lived ^{67}Ga was used throughout the study. The outcomes of this study would also be applicable to the synthesis of ^{68}Ga labeled NOTA-(TEG-RGD)$_3$. Moreover, given the efforts in processing generator eluates to reduce metal impurities[5,45−47] and the sensitivity of PET imaging techniques, superior images of in vivo integrin $\alpha_v\beta_3$ expression can be obtained.

CONCLUSIONS

The findings in this study show that the RGD conjugates of both diastereomers presented here possess equivalent biological efficacy, and the combined usage of the diastereomic mixture would be feasible as far as the present compounds are concerned. It is worth noting that the specific properties of a given biomolecule, cell expression levels of the corresponding target molecule, and presence or absence of pharmacokinetic modifier might affect the structural differences between diastereomers on the ligand−receptor interactions and biodistribution. Since the synthesis of diastereomerically pure NOTGA-^{t}Bu prochelators has been established, the preparation of corresponding conjugates and evaluation of their chemical and biological performances still remains important for applying NOTGA to other biomolecules of interest.

ASSOCIATED CONTENT

Supporting Information

^{1}H and ^{13}C NMR and LC-MS spectra of the diastereomeric pairs of NOTGA-^{t}Bu$_3$-Bz$_3$. This material is available free of charge via the Internet at http://pubs.acs.org.

AUTHOR INFORMATION

Corresponding Author

*Tel: +81-43-256-1782. Fax: +81-43-226-2897. E-mail: arano@chiba-u.jp.

Notes

The authors declare no competing financial interest.

■ ACKNOWLEDGMENTS

This work was partially supported by Special Funds for Education and Research (Development of SPECT Probes for Pharmaceutical Innovation) from the Ministry of Education, Culture, Sports, Science and Technology, Japan. We would also like to thank FUJIFILM RI Pharma Co., Ltd. for providing [^{67}Ga]Cl_3.

■ REFERENCES

(1) Fani, M., André, J. P., and Maecke, H. R. (2008) ^{68}Ga-PET: a powerful generator-based alternative to cyclotron-based PET radiopharmaceuticals. *Contr. Media Mol. Imaging 3*, 67−77.

(2) Green, M. A., and Welch, M. J. (1989) Gallium radiopharmaceutical chemistry. *Int. J. Radiat. Appl. Instrum. Part B 16*, 435−443 445−448.

(3) Weiner, R. E. (1996) The mechanism of ^{67}Ga localization in malignant disease. *Nucl. Med. Biol. 23*, 745−751.

(4) Clarke, E. T., and Martell, A. E. (1991) Stabilities of the Fe(III), Ga(III) and In(III) chelates of N,N′,N″-triazacyclononanetriacetic acid. *Inorg. Chim. Acta 181*, 273−280.

(5) Ferreira, C. L., Lamsa, E., Woods, M., Duan, Y., Fernando, P., Bensimon, C., Kordos, M., Guenther, K., Jurek, P., and Kiefer, G. E. (2010) Evaluation of bifunctional chelates for the development of gallium-based radiopharmaceuticals. *Bioconjugate Chem. 21*, 531−536.

(6) Jae, M. J., Mee, K. H., Young, S. C., Lee, Y. S., Young, J. K., Gi, J. C., Dong, S. L., Chung, J. K., and Myung, C. L. (2008) Preparation of a promising angiogenesis PET imaging agent: ^{68}Ga-labeled c-(RGDyK)-isothiocyanatobenzyl-1,4,7-triazacyclononane-1, 4,7-triacetic acid and feasibility studies in mice. *J. Nucl. Med. 49*, 830−836.

(7) Velikyan, I., Maecke, H., and Langstrom, B. (2008) Convenient preparation of ^{68}Ga-based PET-radiopharmaceuticals at room temperature. *Bioconjugate Chem. 19*, 569−573.

(8) André, J. P., Maecke, H. R., Zehnder, M., Macko, L., and Akyel, K. G. (1998) 1,4,7-Triazacyclononane-1-succinic acid-4,7-diacetic acid (NODASA): A new bifunctional chelator for radio gallium-labelling of biomolecules. *Chem. Commun.*, 1301−1302.

(9) Riss, P. J., Kroll, C., Nagel, V., and Rösch, F. (2008) NODAPA-OH and NODAPA-(NCS)n: Synthesis, ^{68}Ga-radiolabelling and in vitro characterisation of novel versatile bifunctional chelators for molecular imaging. *Bioorg. Med. Chem. Lett. 18*, 5364−5367.

(10) Eisenwiener, K. P., Prata, M. I. M., Buschmann, I., Zhang, H. W., Santos, A. C., Wenger, S., Reubi, J. C., and Mäcke, H. R. (2002) NODAGATOC, a new chelator-coupled somatostatin analogue labeled with [$^{67/68}$Ga] and [^{111}In] for SPECT, PET, and targeted therapeutic applications of somatostatin receptor (hsst2) expressing tumors. *Bioconjugate Chem. 13*, 530−541.

(11) Notni, J., Hermann, P., Havlíčková, J., Kotek, J., Kubíček, V., Plutnar, J., Loktionova, N., Riss, P. J., Rösch, F., and Lukeš, I. (2010) A triazacyclononane-based bifunctional phosphinate ligand for the preparation of multimeric ^{68}GA tracers for positron emission tomography. *Chem.—Eur. J. 16*, 7174−7185.

(12) Notni, J., Šimeček, J., Hermann, P., and Wester, H. J. (2011) TRAP, a powerful and versatile framework for gallium-68 radiopharmaceuticals. *Chem.—Eur. J. 17*, 14718−14722.

(13) Uehara, T., Guerra Gomez, F. L., Rokugawa, T., and Arano, Y. (2011) A new triazacyclononane-based ligand for trivalent ^{68}Ga tracers of high stability for positron emission tomography. *J. Nucl. Med. 52*, 1473.

(14) Singh, A. N., Liu, W., Hao, G., Kumar, A., Gupta, A.O. Z O. K., Hsieh, J.-T., and Sun, X. (2011) Multivalent bifunctional chelator scaffolds for gallium-68 based positron emission tomography imaging probe design: signal amplification via multivalency. *Bioconjugate Chem. 22*, 1650−1662.

(15) Abiraj, K., Jaccard, H., Kretzschmar, M., Helm, L., and Maecke, H. R. (2008) Novel DOTA-based prochelator for divalent peptide vectorization: Synthesis of dimeric bombesin analogues for multimodality tumor imaging and therapy. *Chem. Commun.*, 3248−3250.

(16) Woods, M., Aime, S., Botta, M., Howard, J. A. K., Moloney, J. M., Navet, M., Parker, D., Port, M., and Rousseaux, O. (2000) Correlation of water exchange rate with isomeric composition in diastereoisomeric gadolinium complexes of tetra(carboxyethyl)dota and related macrocyclic ligands. *J. Am. Chem. Soc. 122*, 9781−9792.

(17) Šimeček, J., Schulz, M., Notni, J., Plutnar, J., Kubíček, V., Havlíčková, J., and Hermann, P. (2012) Complexation of metal ions with TRAP (1,4,7-triazacyclononane phosphinic acid) ligands and 1,4,7-triazacyclononane-1,4,7-triacetic acid: Phosphinate-containing ligands as unique chelators for trivalent gallium. *Inorg. Chem. 51*, 577−590.

(18) Cantorias, M. V., Howell, R. C., Todaro, L., Cyr, J. E., Berndorff, D., Rogers, R. D., and Francesconi, L. C. (2007) MO tripeptide diastereomers (M = $^{99/99m}$Tc, Re): models to identify the structure of ^{99m}Tc peptide targeted radiopharmaceuticals. *Inorg. Chem. 46*, 7326−7340.

(19) Cyr, J. E., Pearson, D. A., Nelson, C. A., Lyons, B. A., Zheng, Y., Bartis, J., He, J., Cantorias, M. V., Howell, R. C., and Francesconi, L. C. (2007) Isolation, characterization, and biological evaluation of syn and anti diastereomers of [^{99m}Tc]technetium depreotide: a somatostatin receptor binding tumor imaging agent. *J. Med. Chem. 50*, 4295−4303.

(20) Haubner, R., Wester, H. J., Reuning, U., Senekowitsch-Schmidtke, R., Diefenbach, B., Kessler, H., Stöcklin, G., and Schwaiger, M. (1999) Radiolabeled $\alpha v\beta 3$ integrin antagonists: A new class of tracers for tumor targeting. *J. Nucl. Med. 40*, 1061−1071.

(21) Eisenwiener, K. P., Powell, P., and Mäcke, H. R. (2000) A convenient synthesis of novel bifunctional prochelators for coupling to bioactive peptides for radiometal labelling. *Bioorg. Med. Chem. Lett. 10*, 2133−2135.

(22) Imai, S., Morimoto, J., Tsubura, Y., Esaki, K., Michalides, R., Holmes, R. S., von Deimling, O., and Hilgers, J. (1986) Genetic marker patterns and endogenous mammary tumor virus genes in inbred mouse strains of Japan. *Exp. Anim. 35*, 263−273.

(23) Pierrard, J. C., Rimbault, J., Aplincourt, M., Le Greneur, S., and Port, M. (2008) New synthesis of a high molecular weight ligand derived from dota; thermodynamic stability of the MRI contrast agent formed with gadolinium. *Contr. Media Mol. Imaging 3*, 243−252.

(24) Liu, S. (2009) Radiolabeled cyclic RGD peptides as integrin $\alpha v\beta 3$-targeted radiotracers: Maximizing binding affinity via bivalency. *Bioconjugate Chem. 20*, 2199−2213.

(25) Chen, X., Tohme, M., Park, R., Hou, Y., Bading, J. R., and Conti, P. S. (2004) Micro-PET imaging of $\alpha v\beta 3$-integrin expression with^{18}F-labeled dimeric RGD peptide. *Mol. Imaging 3*, 96−104.

(26) Dijkgraaf, I., Yim, C.-B., Franssen, G., Schuit, R., Luurtsema, G., Liu, S., Oyen, W., and Boerman, O. (2011) PET imaging of $\alpha v\beta 3$ integrin expression in tumours with ^{68}Ga-labelled mono-, di- and tetrameric RGD peptides. *Eur. J. Nucl. Med. Mol. Imaging 38*, 128−137.

(27) Li, Z. B., Chen, K., and Chen, X. (2008) ^{68}Ga-labeled multimeric RGD peptides for microPET imaging of integrin $\alpha v\beta 3$ expression. *Eur. J. Nucl. Med. Mol. Imaging 35*, 1100−1108.

(28) Liu, S. (2006) Radiolabeled multimeric cyclic RGD peptides as integrin $\alpha v\beta 3$ targeted radiotracers for tumor imaging. *Mol. Pharmaceutics 3*, 472−487.

(29) Jia, B., Liu, Z., Shi, J., Yu, Z., Yang, Z., Zhao, H., He, Z., Liu, S., and Wang, F. (2008) Linker effects on biological properties of ^{111}In-labeled DTPA conjugates of a cyclic RGDfK dimer. *Bioconjugate Chem. 19*, 201−210.

(30) Chen, X., Park, R., Shahinian, A. H., Bading, J. R., and Conti, P. S. (2004) Pharmacokinetics and tumor retention of ^{125}I-labeled RGD peptide are improved by PEGylation. *Nucl. Med. Biol. 31*, 11−19.

(31) Moore, D. A., Fanwick, P. E., and Welch, M. J. (1990) A novel hexachelating amino-thiol ligand and its complex with gallium(III). *Inorg. Chem. 29*, 672−676.

(32) Bandoli, G., Dolmella, A., Tisato, F., Porchia, M., and Refosco, F. (2009) Mononuclear six-coordinated Ga(III) complexes: A comprehensive survey. *Coord. Chem. Rev. 253*, 56−77.

(33) Knetsch, P. A., Petrik, M., Griessinger, C. M., Rangger, C., Fani, M., Kesenheimer, C., Von Guggenberg, E., Pichler, B. J., Virgolini, I., Decristoforo, C., and Haubner, R. (2011) NODAGA-RGD for

imaging $\alpha v\beta 3$ integrin expression. *Eur. J. Nucl. Med. Mol. Imaging 38*, 1303−1312.
(34) Morfin, J. F., and Tóth, E. (2011) Kinetics of Ga(NOTA) formation from weak Ga-citrate complexes. *Inorg. Chem. 50*, 10371−10378.
(35) Brucher, E., and Sherry, A. D. (1990) Kinetics of formation and dissociation of the 1,4,7-triazacyclononnonane-N,N,′,N,″-triacetate complexes of cerium(III), gadolinium(III), and erbium(III) ions. *Inorganic Chem. 29*, 1555−1559.
(36) Chang, C. A., Liu, Y. L., Chen, C. Y., and Chou, X. M. (2001) Ligand preorganization in metal ion complexation: Molecular mechanics/dynamics, kinetics, and laser-excited luminescence studies of trivalent lanthanide complex formation with macrocyclic ligands TETA and DOTA. *Inorg. Chem. 40*, 3448−3455.
(37) Moreau, J., Guillon, E., Pierrard, J. C., Rimbault, J., Port, M., and Aplincourt, M. (2004) Complexing mechanism of the lanthanide cations Eu^{3+}, Gd^{3+}, and Tb^{3+} with 1,4,7,10-tetrakis (carboxymethyl)-1,4,7, 10-tetraazacyclododecane (dota) - characterization of three successive complexing phases: Study of the thermodynamic and structural properties of the complexes by potentiometry, luminescence spectroscopy, and EXAFS. *Chem.—Eur. J. 10*, 5218−5232.
(38) Wang, L., Shi, J., Kim, Y.-S., Zhai, S., Jia, B., Zhao, H., Liu, Z., Wang, F., Chen, X., and Liu, S. (2008) Improving tumor-targeting capability and pharmacokinetics of ^{99m}Tc-labeled cyclic RGD dimers with PEG4 linkers. *Mol. Pharmaceutics 6*, 231−245.
(39) Liu, Z., Niu, G., Shi, J., Liu, S., Wang, F., and Chen, X. (2009) ^{68}Ga-labeled cyclic RGD dimers with Gly3 and PEG4 linkers: Promising agents for tumor integrin α v$\beta 3$ PET imaging. *Eur. J. Nucl. Med. Mol. Imaging 36*, 947−957.
(40) Li, Z. B., Cai, W., Cao, Q., Chen, K., Wu, Z., He, L., and Chen, X. (2007) ^{64}Cu-labeled tetrameric and octameric RGD peptides for small-animal PET of tumor $\alpha v\beta 3$ integrin expression. *J. Nucl. Med. 48*, 1162−1171.
(41) Garanger, E., Boturyn, D., Coll, J.-L., Favrot, M.-C., and Dumy, P. (2006) Multivalent RGD synthetic peptides as potent $\alpha v\beta 3$ integrin ligands. *Org. Biomol. Chem. 4*, 1958−1965.
(42) Wu, Y., Zhang, X., Xiong, Z., Cheng, Z., Fisher, D. R., Liu, S., Gambhir, S. S., and Chen, X. (2005) microPET imaging of glioma integrin $\alpha v\beta 3$ expression using ^{64}Cu-labeled tetrameric RGD peptide. *J. Nucl. Med. 46*, 1707−1718.
(43) Wu, Z., Li, Z.-B., Chen, K., Cai, W., He, L., Chin, F. T., Li, F., and Chen, X. (2007) microPET of tumor integrin $\alpha v\beta 3$ expression using ^{18}F-labeled PEGylated tetrameric RGD peptide (^{18}F-FPRGD4). *J. Nucl. Med. 48*, 1536−1544.
(44) Akizawa, H., Uehara, T., and Arano, Y. (2008) Renal uptake and metabolism of radiopharmaceuticals derived from peptides and proteins. *Adv. Drug Delivery Rev. 60*, 1319−1328.
(45) Breeman, W. A. P., De Jong, M., De Blois, E., Bernard, B. F., Konijnenberg, M., and Krenning, E. P. (2005) Radiolabelling DOTA-peptides with ^{68}Ga. *Eur. J. Nucl. Med. Mol. Imaging 32*, 478−485.
(46) Loktionova, N. S., Belozub, A. N., Filosofov, D. V., Zhernosekov, K. P., Wagner, T., Türler, A., and Rösch, F. (2011) Improved column-based radiochemical processing of the generator produced ^{68}Ga. *Appl. Radiat. Isot. 69*, 942−946.
(47) Tolmachev, V., and Stone-Elander, S. (2010) Radiolabelled proteins for positron emission tomography: Pros and cons of labelling methods. *Biochim. Biophys. Acta 1800*, 487−510.